

Statistical methods for analyzing spatially-referenced paired genetic relatedness data

Joshua L. Warren^{1*}, Melanie H. Chitwood², Benjamin Sobkowiak³,
Valeriu Crudu⁴, Caroline Colijn³, Ted Cohen²

¹Department of Biostatistics, Yale University, New Haven, CT 06510, USA

²Department of Epidemiology of Microbial Diseases, Yale University, New Haven, CT 06510, USA

³Department of Mathematics, Simon Fraser University, Burnaby, BC V5A 1S6, CA

⁴Microbiology and Morphology Laboratory, Phthisiopneumology Institute, Chisinau, MLD

Abstract

Understanding factors that contribute to the increased likelihood of disease transmission between two individuals is important for infection control. Measures of genetic relatedness of bacterial isolates between two individuals are often analyzed to determine their associations with these factors using simple correlation or regression analyses. However, these standard approaches ignore the potential for correlation in paired data of this type, arising from the presence of the same individual across multiple paired outcomes. We develop two novel hierarchical Bayesian methods for properly analyzing paired genetic relatedness data in the form of patristic distances and transmission probabilities. Using individual-level spatially correlated random effect parameters, we account for multiple sources of correlation in the outcomes as well as other important features of their distribution. Through simulation, we show that the standard analyses drastically underestimate uncertainty in the associations when correlation is present in the data, leading to incorrect conclusions regarding the covariates of interest. Conversely, the newly developed methods perform well under various levels of correlated and

*This work was supported in part by the National Institute of Allergy and Infectious Diseases (R01 AI147854, R01 AI137093) and the generous support of the American people through the United States Agency for International Development (USAID) through the TREAT TB Cooperative Agreement No. GHN-A-00-08-00004. The contents are the responsibility of the authors and Subgrantee and do not necessarily reflect the views of USAID or the United States Government.

uncorrelated data. All methods are applied to *Mycobacterium tuberculosis* data from the Republic of Moldova where we identify factors associated with disease transmission and, through analysis of the random effect parameters, key individuals and areas with increased transmission activity. Model comparisons show the importance of the new methodology in this setting. The methods are implemented in the R package **GenePair**.

Keywords: Hierarchical Bayesian methods; Patristic distance; Phylogenetic tree; Spatial statistics; Transmission probability.

1 Introduction

The availability and affordability of whole-genome sequencing technology has made the use of genomic data increasingly common in epidemiological modeling studies (Loman and Pallen, 2015; Polonsky et al., 2019). Sequencing data from bacteriological pathogens provide insight into the spread of infectious diseases through populations and numerous methods have been developed to infer person-to-person transmission. The simplest approach uses the difference of single nucleotide polymorphisms (SNPs) between two samples and assigns any pairs separated by fewer than a threshold number of SNPs to a transmission cluster (Walker et al., 2014). Other approaches make use of phylogenetic trees, a reconstruction of the estimated evolutionary history of a pathogen based on genetic sequencing data (Delsuc et al., 2005). For example, patristic distances, the summed length of the tree branches separating two isolates, is a similar measure of genetic distance, but this approach leverages prior biological assumptions about the substitution rate to generate a more accurate measure than SNP distance (Poon, 2016). More complex approaches make use of transmission trees, based on phylogenetic analyses, to estimate the asymmetric probability of direct transmission between pairs of cases (Didelot et al., 2017; Klinkenberg et al., 2017; Campbell et al., 2019).

While a robust set of methods exists to estimate genetic relatedness between case pairs, statistical methods to analyze these paired data and their associations with other factors are limited. However, understanding how potentially modifiable factors contribute to the increased likelihood of disease transmission between two individuals is important for infection control. Frequently, researchers report correlation estimates between genetic relatedness and another covariate, such as the geographic distance separating cases (Alberto et al., 2005; Lieberman et al., 2016; Gates et al., 2019). Another common approach is to perform a multiple linear regression analysis with the paired genetic relatedness measure as the outcome variable and characteristics of individuals within the pair as predictors (Vekemans and Hardy, 2004; Kitchen et al., 2005; Omedo et al., 2017; Sy et al., 2020).

These approaches to analyzing paired genetic relatedness data have several limitations. Potentially the most serious concern is that they do not account for correlation in the paired outcome due to the fact that the same individual is represented across multiple pairs. For example, we may expect correlation between paired outcomes Y_{ij} and Y_{kj} , describing the genetic relatedness between individuals i, j and k, j respectively, because individual j is present in both pairs; particularly if individual j is a major driver of transmission in the population. Ignoring this potentially positive correlation during analysis can result in overly optimistic measures of uncertainty for regression parameter estimates, leading to incorrect conclusions regarding statistical significance. Basic regression approaches currently being used can also oversimplify important features of the data (e.g., zero-inflation, non-Gaussian distribution) and ignore other sources of correlation (e.g., spatial correlation due to unmeasured transmission dynamics), all of which may impact statistical inference for the regression parameters of interest.

In this work, we develop innovative hierarchical Bayesian methods for properly analyzing paired genetic relatedness data in the form of patristic distances and transmission probabilities. Our framework overcomes limitations of existing approaches by accounting for correlation between the paired outcomes, correctly modeling the appropriate distribution of the data, and adjusting for spatial correlation between outcomes; all while simultaneously estimating the associations between genetic relatedness and covariates of interest. Using a simulation study, we show the importance of these methods for conducting accurate statistical inference on key regression associations and the limitations of an existing approach. We also apply our methods to a unique dataset describing *Mycobacterium tuberculosis* transmission dynamics in the Republic of Moldova and show the benefits of the new methodology with respect to inference and model fit. Analyzing the posterior distributions of person-specific random effect parameters is shown to be important for understanding how individuals in the population personally contribute to the transmission dynamics and the role of spatial versus individual variability in this process. Given the increasing availability and interest in these types of data, and the limitations of existing approaches, we anticipate that these methods

will represent important tools for researchers looking to correctly identify factors associated with genetic relatedness between individuals in future studies.

In Section 2 we describe the data from the Republic of Moldova while the new statistical methods are presented in Section 3. Sections 4 and 5 represent the simulation study and real data application, respectively. We close in Section 6 with conclusions and further discussion.

2 Data

We utilize data previously described by Yang et al. (2021). To summarize, the authors performed whole genome sequencing on *Mycobacterium tuberculosis* isolates from 2,236 of the 2,770 non-incarcerated adults diagnosed with culture-positive tuberculosis (TB) in the Republic of Moldova between January 1, 2018 and December 31, 2019. The authors constructed a maximum likelihood phylogenetic tree with RAxML (Stamatakis, 2014) and identified broad, putative transmission clusters using TreeCluster (Balaban et al., 2019) with a threshold of 0.001 substitutions per site. Clusters with 10 or more individuals were included in an additional analysis to reconstruct transmission networks using the TransPhylo “multi-tree” method (Didelot et al., 2017).

From these analyses, Yang et al. (2021) produced estimates of genetic relatedness among sequences using two metrics. First, they computed patristic distance between any pair of isolates within a cluster. Patristic distance is a measure of genetic relatedness between two sequences in a phylogenetic tree expressed in substitutions per site. Second, the authors estimated the probability that one individual infected another individual. These probabilities are obtained using a Bayesian approach (TransPhylo) that augments timed phylogenetic trees with who-infected-whom information, accounting for the possibility of unsampled individuals. TransPhylo uses a Markov chain Monte Carlo (MCMC) framework to obtain a posterior collection of transmission trees, accounting for the time from infection to infecting others (generation time) and the time from infection to sampling. For most pairs (i, j) , there is no posterior transmission tree that includes a transmission event from i to j or from j to i . Where there are samples in the posterior in which i or j in-

Table 1: Summarizing characteristics of the paired genetic relatedness responses in the Republic of Moldova study population by transmission probability (TP) status. Means, with interquartile ranges given in parentheses, are shown for continuous variables and percentages are shown for categorical variables.

Effect	TP = 0 ($n = 6,958$)	TP > 0 ($n = 2,744$)
Distance Between Villages (km)	87.49 (67.92)	94.76 (78.13)
Same Village (% Yes)	0.56	1.28
Date of Diagnosis Difference (Day)	225.09 (233.75)	202.41 (211.00)
Age Difference (Year)	13.57 (14.00)	13.33 (15.00)
Sex (%):		
Both Male	56.54	58.89
Both Female	6.11	4.63
Mixed Pair	37.35	36.48
Residence Location (%):		
Both Urban	14.62	14.18
Both Rural	37.55	38.16
Mixed Pair	47.83	47.67
Working Status (%):		
Both Employed	0.99	0.77
Both Unemployed	80.81	80.50
Mixed Pair	18.19	18.73
Education (%):		
Both < Secondary	10.30	10.02
Both \geq Secondary	45.33	46.21
Mixed Pair	44.37	43.77

fecting the other, the posterior probability is not symmetric. This can occur, for example, because i was sampled many months prior to j , making it more likely that i infected j than vice versa.

For all possible pairs within a transmission cluster, symmetric estimates of patristic distance (i.e., $Y_{ij} = Y_{ji}$) and asymmetric estimates of transmission probability (i.e., $Y_{ij} \neq Y_{ji}$ necessarily) are available.

In addition to estimates of genetic relatedness, demographic data are available for each TB case. These data include individual characteristics such as age (in years), sex, education status (less than secondary, secondary or higher), working status (employed, unemployed), and residence type (urban, not urban). With these data, we calculate characteristics of the pair of individuals, such as an indicator for whether the individuals in the pair reside in the same village, the Euclidean distance between their villages of residence (in kilometers), the difference between their dates of diagnosis (in days), and the absolute difference between their ages (in years).

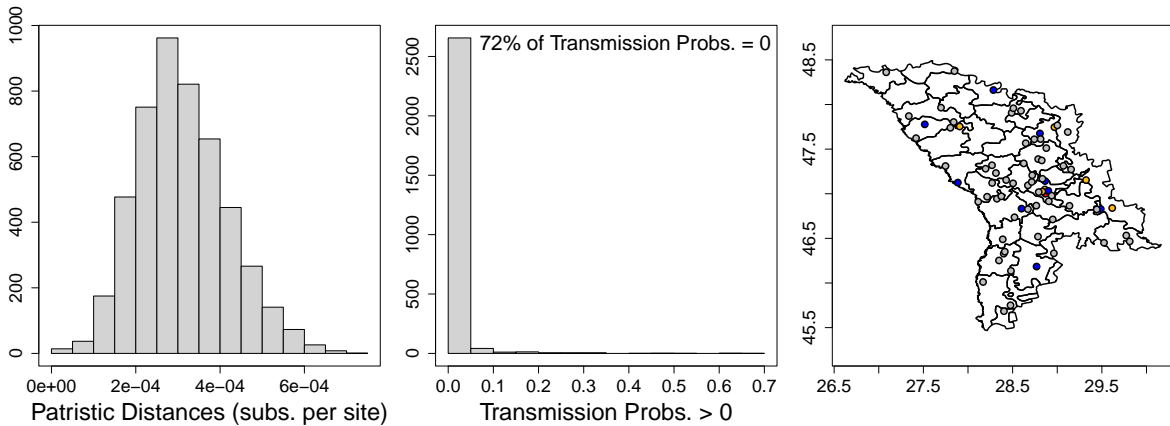


Figure 1: Patristic distances (substitutions per site; panel 1), transmission probabilities that are > 0 (panel 2), and village locations (panel 3) from the largest putative cluster in the Republic of Moldova data analysis. In panel 3, gray, blue, orange, and red points represent villages with one, two, three, and five cases, respectively.

We illustrate the introduced statistical methods with the largest putative transmission cluster in the dataset. After removing six individuals with missing covariates, the final analysis dataset

includes 99 individuals resulting in 4,851 symmetric patristic distance pairs and 9,702 asymmetric transmission probability pairs. Characteristics of the paired data from this specific cluster are shown in Table 1 while in Figure 1 we display distributions of the different genetic relatedness outcomes along with the village locations for individuals in the study.

3 Methods

We develop models to properly analyze paired genetic relatedness outcomes (i.e., patristic distances, transmission probabilities) while accounting for multiple sources of correlation between responses and important features of the outcomes. The methods are designed to yield accurate statistical inference for the primary regression associations of interest while also identifying individuals/locations that play a more important role in the transmission dynamics within the population.

3.1 Patristic distances

We model the patristic distance (log scale) between persons i and j as a function of pair- and individual-level covariates as well as spatially-referenced, person-specific random effects such that

$$\ln(Y_{ij}) = \mathbf{x}_{ij}^T \boldsymbol{\beta} + (\mathbf{d}_i + \mathbf{d}_j)^T \boldsymbol{\gamma} + \theta_i + \theta_j + \epsilon_{ij}, \quad (1)$$

$i = 1, \dots, n-1$, $j = i+1, \dots, n$, where $\epsilon_{ij} | \sigma_\epsilon^2 \stackrel{\text{iid}}{\sim} \text{N}(0, \sigma_\epsilon^2)$ is the error term; n is the total number of individuals in the study; $Y_{ij} > 0$ is the symmetric patristic distance between a unique pair of individuals i and j (i.e., $Y_{ij} = Y_{ji}$ for all $i \neq j$); \mathbf{x}_{ij} is a vector of covariates describing differences between individuals i and j (e.g., spatial distance), with $\boldsymbol{\beta}$ the corresponding vector of regression parameters; \mathbf{d}_i is a vector of covariates specific to individual i where the impact of the covariates on the response, described by the $\boldsymbol{\gamma}$ vector, is assumed to be the same across all individuals; and θ_i is a spatially-referenced, individual-specific random effect parameter which describes individual i 's role in transmission events within the population (both as infector and infectee). Small θ_i values

indicate that across all outcome pairs involving individual i , the patristic distance is smaller on average, suggestive of an increased likelihood of being in transmission pairs. In Section 3.3 we investigate the correlation induced on the outcomes through use of these parameters.

We allow for the possibility of spatial correlation between responses by modeling the random effect parameters using a spatially-referenced Gaussian process such that

$$\begin{aligned}\theta_i &= \eta \{h(\mathbf{s}_i)\} + \zeta_i, \quad i = 1, \dots, n, \\ \boldsymbol{\eta}^T &= \{\eta(\mathbf{s}_1^*), \dots, \eta(\mathbf{s}_m^*)\} | \phi, \tau^2 \sim \text{MVN} \{ \mathbf{0}_m, \tau^2 \Sigma(\phi) \}, \text{ and} \\ \Sigma(\phi)_{ij} &= \text{Corr} \{ \eta(\mathbf{s}_i^*), \eta(\mathbf{s}_j^*) \} = \exp \{ -\phi \|\mathbf{s}_i^* - \mathbf{s}_j^*\| \}\end{aligned}\tag{2}$$

where θ_i is decomposed into two pieces; one that is purely spatial, $\eta(\mathbf{s}_i^*)$, and one that is non-spatial, ζ_i . This allows for each parameter to be individual-specific and not driven solely by spatial location. In the case where individuals are co-located, the function $h(\cdot)$ maps the spatial location of an individual to an entry within a smaller set of $m < n$ unique locations such that $h(\mathbf{s}_i) \in \{\mathbf{s}_1^*, \dots, \mathbf{s}_m^*\}$, where it is possible that $h(\mathbf{s}_i) = h(\mathbf{s}_j) = \mathbf{s}_k^*$ for some $i \neq j$. When all individuals have a unique location, $h(\mathbf{s}_i) = \mathbf{s}_i^*$ for all i and therefore, $m = n$.

The vector of purely spatial random effects, $\boldsymbol{\eta}$, is modeled using a Gaussian process centered at zero (i.e., $\mathbf{0}_m$ is an m length vector of zeros) with correlation structure defined by the Euclidean distances between spatial locations (i.e., $\|\mathbf{s}_i^* - \mathbf{s}_j^*\|$), where $\phi > 0$ controls the level of spatial correlation between the parameters and τ^2 the total variability of the spatial process. Small values of ϕ indicate strong spatial correlation even at larger distances. Finally, $\zeta_i | \sigma_\zeta^2 \stackrel{\text{iid}}{\sim} \text{N}(0, \sigma_\zeta^2)$ represent the individual-specific parameters that account for the possibility that two people could be in very similar spatial locations but have vastly different patterns of behavior that impact their likelihood of being transmitted to and/or transmitting to others.

3.1.1 Prior distributions

We assign weakly informative prior distributions to the remaining model parameters when appropriate. The regression parameters are specified as $\beta_j, \gamma_k \stackrel{\text{iid}}{\sim} \text{N}(0, 100^2)$ for $j = 1, \dots, p_x$ and

$k = 1, \dots, p_d$, where p_x and p_d are the lengths of the \mathbf{x}_{ij} and \mathbf{d}_i vectors, respectively; the variance parameters as $\sigma_\epsilon^2, \tau^2, \sigma_\zeta^2 \stackrel{\text{iid}}{\sim} \text{Inverse Gamma}(0.01, 0.01)$; and the spatial correlation parameter as $\phi \sim \text{Gamma}(1.00, 1.00)$.

3.2 Transmission probabilities

Next, we introduce a method for analyzing transmission probabilities which, unlike patristic distances, contain potentially rich information regarding the direction of transmission. As a result, the outcomes are not symmetric as they were in Section 3.1 (i.e., $Y_{ij} \neq Y_{ji}$ necessarily). Here, we introduce a framework for properly analyzing transmission probabilities that includes similar inferential goals as the model in (1, 2) while also accounting for the asymmetry of the outcome as well as other important data features (e.g., zero-inflation, non-Gaussian distribution).

Specifically, we model the probability that individual j infected individual i (i.e., Y_{ij}) as a function of individual and pair-specific covariates and individual/location-specific random effect parameters using a mixed-type distribution. This specification includes a binary component to account for the large proportion of exact zero transmission probabilities (see Figure 1), and a continuous piece to model the non-zero probabilities. We define the probability density function (pdf) for a transmission probability, $f_{y_{ij}}(y)$, as

$$Y_{ij} \stackrel{\text{ind}}{\sim} f_{y_{ij}}(y) = (1 - \pi_{ij})^{1(y=0)} \left[\frac{\pi_{ij}}{y(1-y)} f_{w_{ij}} \left\{ \ln \left(\frac{y}{1-y} \right) \right\} \right]^{1(y>0)}, \quad y \in [0, 1] \quad (3)$$

where all pairs are now included in the analysis (i.e., $i = 1, \dots, n; j = 1, \dots, n; i \neq j$); $1(\cdot)$ is an indicator function taking the value of one when the input statement is true and the value of zero otherwise; the transmission probabilities can be exactly equal to zero; and $(1 - \pi_{ij})$ describes the probability that this event occurs.

We use a logistic regression framework to connect these underlying probabilities with covariates and random effect parameters such that

$$\ln \left(\frac{\pi_{ij}}{1 - \pi_{ij}} \right) = \mathbf{x}_{ij}^T \boldsymbol{\beta}_z + \mathbf{d}_j^T \boldsymbol{\gamma}_z^{(g)} + \mathbf{d}_i^T \boldsymbol{\gamma}_z^{(r)} + \theta_{zj}^{(g)} + \theta_{zi}^{(r)} \quad (4)$$

where \mathbf{x}_{ij} and \mathbf{d}_i were previously described in Section 3.1. Because we now observe two responses for each pair (i.e., Y_{ij} and Y_{ji}), we are able to separate the included parameters into the different roles of the individuals within a pair; specifically, we can estimate the infector or “giver” (g) and the infectee or “receiver” (r) terms. For example, Y_{ij} describes the probability that individual j transmits to i , so $\mathbf{d}_j^T \boldsymbol{\gamma}_z^{(g)}$ from (4) represents the impact of the giver’s (individual j ’s) covariates on the probability of transmission while $\mathbf{d}_i^T \boldsymbol{\gamma}_z^{(r)}$ describes the impact of the receiver’s (individual i ’s) characteristics. Similarly, now each individual has two different random effect parameters for this regression model, $\boldsymbol{\theta}_{zi}^T = (\theta_{zi}^{(g)}, \theta_{zi}^{(r)})$; one for the giver and receiver roles, respectively.

In order to understand if the magnitude of a non-zero transmission probability is also impacted by covariates and random effect parameters, the pdf in (3) includes a separate regression framework for the non-zero probabilities. Specifically, $f_{wij}(w)$ is a pdf introduced to model the non-zero probabilities on the logit scale such that

$$f_{wij}(w) \equiv N\left(\mathbf{x}_{ij}^T \boldsymbol{\beta}_w + \mathbf{d}_j^T \boldsymbol{\gamma}_w^{(g)} + \mathbf{d}_i^T \boldsymbol{\gamma}_w^{(r)} + \theta_{wj}^{(g)} + \theta_{wi}^{(r)}, \sigma_\epsilon^2\right) \quad (5)$$

where σ_ϵ^2 represents the variance of the distribution and the remaining terms in (5) have been previously described. The “ w ” subscripts in (5) serve to differentiate these parameters from those used by the binary model in (4) (i.e., “ z ” subscripts).

In total, each individual in the analysis has four random effect parameters, $\boldsymbol{\theta}_i^T = (\boldsymbol{\theta}_{zi}^T, \boldsymbol{\theta}_{wi}^T)$, representing the residual (i.e., after adjustment for known risk factors) likelihood of transmitting (g) or being transmitted to (r) in the binary (z) and positive (w) transmission probability regressions. Large values of the z subscript random effect parameters suggest an increased chance of a non-zero transmission probability, while large values of the w subscript parameters indicate an increasingly positive transmission probability.

As in (2), the introduced random effect parameters serve to adjust for pair- and proximity-based correlation in the outcomes. We anticipate that the collection of parameters corresponding to the same individual may themselves be correlated and introduce a multivariate model as a result. The

model for one set of the parameters is similar to (2) and is given as (for $i = 1, \dots, n$)

$$\theta_{zi}^{(g)} = \eta_z^{(g)} \{h(\mathbf{s}_i)\} + \zeta_{zi}^{(g)}$$

where $\zeta_{zi}^{(g)} | \sigma_{\zeta_z^{(g)}}^2 \stackrel{\text{iid}}{\sim} \text{N}(0, \sigma_{\zeta_z^{(g)}}^2)$ once again account for individual variability, and the remaining parameters, $\theta_{zi}^{(r)}$, $\theta_{wi}^{(g)}$, $\theta_{wi}^{(r)}$, are defined similarly. To account for cross-covariance and spatial correlation among the parameters, we specify a multivariate Gaussian process for the mean parameters such that

$$\begin{aligned} \boldsymbol{\eta} | \Omega, \phi &\sim \text{MVN} \{ \mathbf{0}_{4m}, \Sigma(\phi) \otimes \Omega \} \text{ where} \\ \boldsymbol{\eta}^T &= \left\{ \boldsymbol{\eta}(\mathbf{s}_1^*)^T, \dots, \boldsymbol{\eta}(\mathbf{s}_m^*)^T \right\} \text{ and} \\ \boldsymbol{\eta}(\mathbf{s}_i^*)^T &= \{ \eta_z^{(g)}(\mathbf{s}_i^*), \eta_z^{(r)}(\mathbf{s}_i^*), \eta_w^{(g)}(\mathbf{s}_i^*), \eta_w^{(r)}(\mathbf{s}_i^*) \}. \end{aligned}$$

The complete collection of mean parameters across all m unique spatial locations is denoted by $\boldsymbol{\eta}$ (similar to (2)); $\boldsymbol{\eta}(\mathbf{s}_i^*)$ represents the collection of mean parameters across each component of the model and different roles, specific to unique location \mathbf{s}_i^* ; $\Sigma(\phi)$ was previously described in (2); \otimes is the Kronecker product; and Ω represents a four-by-four unstructured covariance matrix describing the cross-covariance among the set of four random effect parameters specific to a unique spatial location.

3.2.1 Prior distributions

We complete the model specification by assigning prior distributions to the introduced model parameters. As in Section 3.1.1, the regression parameters are specified as β_{zj} , β_{wj} , $\gamma_{zk}^{(g)}$, $\gamma_{zk}^{(r)}$, $\gamma_{wk}^{(g)}$, $\gamma_{wk}^{(r)} \stackrel{\text{iid}}{\sim} \text{N}(0, 100^2)$ for $j = 1, \dots, p_x$ and $k = 1, \dots, p_d$; the variance parameters as σ_ϵ^2 , $\sigma_{\zeta_z^{(g)}}^2$, $\sigma_{\zeta_z^{(r)}}^2$, $\sigma_{\zeta_w^{(g)}}^2$, $\sigma_{\zeta_w^{(r)}}^2 \stackrel{\text{iid}}{\sim} \text{Inverse Gamma}(0.01, 0.01)$; the spatial correlation parameter as $\phi \sim \text{Gamma}(1.00, 1.00)$; and the cross-covariance matrix as $\Omega^{-1} \sim \text{Wishart}(5, I_4)$, resulting in uniform cross correlations *a priori* (Gelman et al., 2013).

3.3 Induced correlation structure

The inclusion of individual-specific and spatially correlated random effect parameters in the models for paired outcomes detailed in Sections 3.1 and 3.2 results in a positive correlation between the responses whose magnitude varies depending on (i) if the two pairs share a common person and (ii) the geographic distance between the people in the pairs. To better understand the induced variances, covariances, and correlations, we consider two different cases specifically for the paired patristic distance data; when there is, and is not, a shared individual between the pairs. Correlation calculations for the transmission probability model are similar but more complicated due to the mixed-type distribution and multiple regression frameworks used.

First, we derive the covariance/correlation between two paired patristic distances that consist of entirely different individuals, Y_{ij} and Y_{kl} where $i \neq j \neq k \neq l$, based on the model described in (1, 2). The variance of one of the responses (assuming every individual in the study has a unique spatial location) is given as

$$\begin{aligned} \text{Var} \{ \ln(Y_{ij}) \} &= \text{Var}(\theta_i) + \text{Var}(\theta_j) + \text{Var}(\epsilon_{ij}) + 2\text{Cov}(\theta_i, \theta_j) \\ &= \text{Var} \{ \eta(\mathbf{s}_i^*) + \zeta_i \} + \text{Var} \{ \eta(\mathbf{s}_j^*) + \zeta_j \} + \text{Var}(\epsilon_{ij}) + 2\text{Cov} \{ \eta(\mathbf{s}_i^*) + \zeta_i, \eta(\mathbf{s}_j^*) + \zeta_j \} \\ &= 2\tau^2 (1 + \exp \{ -\phi \|\mathbf{s}_i^* - \mathbf{s}_j^*\| \}) + 2\sigma_\zeta^2 + \sigma_\epsilon^2 \end{aligned}$$

due to the spatial dependence between the θ_i parameters. This suggests that the variability of the responses for individuals separated by large distances may be smaller than for those individuals who are nearby each other. This may be reasonable if we expect that generally individuals further apart are less likely to transmit to each other and therefore, consistently have larger patristic distances. For individuals located closer together, these patristic distances could still be large or small depending on individual behavior related to transmission, resulting in more variability in the distribution.

The covariance between these responses is given as

$$\begin{aligned}
\text{Cov} \{ \ln(Y_{ij}), \ln(Y_{kl}) \} &= \text{E} \{ (\theta_i + \theta_j) (\theta_k + \theta_l) \} \\
&= \text{E} \left[\{ \eta(\mathbf{s}_i^*) + \zeta_i + \eta(\mathbf{s}_j^*) + \zeta_j \} \{ \eta(\mathbf{s}_k^*) + \zeta_k + \eta(\mathbf{s}_l^*) + \zeta_l \} \right] \\
&= \tau^2 \sum_{p_1 \in \{i,j\}} \sum_{p_2 \in \{k,l\}} \exp \{ -\phi \|\mathbf{s}_{p_1}^* - \mathbf{s}_{p_2}^*\| \},
\end{aligned}$$

and is simply a function of spatial distances between the individuals in the pairs. This reasonably suggests that if there is no spatial correlation (or if spatial correlation is negligible) in the parameters, that the covariance/correlation between outcome pairs without a shared individual is effectively equal to zero since $\exp \{ -\phi \|\mathbf{s}_i^* - \mathbf{s}_j^*\| \} \approx 0$ for all i, j . In the case of strong spatial correlation, or people separated by small distances (i.e., $\exp \{ -\phi \|\mathbf{s}_i^* - \mathbf{s}_j^*\| \} \approx 1$), the variance and covariance become $4\tau^2 + 2\sigma_\zeta^2 + \sigma_\epsilon^2$ and $4\tau^2$, respectively. This yields a correlation between the paired outcomes of

$$\frac{4\tau^2}{4\tau^2 + 2\sigma_\zeta^2 + \sigma_\epsilon^2},$$

suggesting the potential for high correlation between responses depending on the magnitudes of the different variance parameters.

Following similar derivations, the covariance between observations for two pairs that include one of the same individuals, say $\ln(Y_{ij})$ and $\ln(Y_{ik})$ (i.e., person i shared), is given as

$$\tau^2 (1 + \exp \{ -\phi \|\mathbf{s}_i^* - \mathbf{s}_j^*\| \} + \exp \{ -\phi \|\mathbf{s}_i^* - \mathbf{s}_k^*\| \} + \exp \{ -\phi \|\mathbf{s}_j^* - \mathbf{s}_k^*\| \}) + \sigma_\zeta^2.$$

Under negligible spatial correlation, this expression approaches $\tau^2 + \sigma_\zeta^2 > 0$ due to the fact that the same person is represented in both pairs; while for strong spatial dependency, it approaches $4\tau^2 + \sigma_\zeta^2$. This yields correlations of

$$\frac{\tau^2 + \sigma_\zeta^2}{2\tau^2 + 2\sigma_\zeta^2 + \sigma_\epsilon^2} \text{ and } \frac{4\tau^2 + \sigma_\zeta^2}{4\tau^2 + 2\sigma_\zeta^2 + \sigma_\epsilon^2}$$

for the weak and strong spatial correlation settings, respectively. Therefore, when the pairs share a common individual, there is a positive correlation between patristic distances regardless of the level of spatial correlation in the parameters.

4 Simulation study

We design a simulation study to investigate the implications of ignoring correlation between paired genetic relatedness outcomes when making inference on regression parameters of interest. Additionally, we aim to better understand how our new methods perform when the correlation structure is misspecified, and if a common Bayesian model comparison tool can be used to identify datasets that contain non-negligible levels of correlation. The process described throughout Section 4 is specifically for the patristic distances model, but we carried out the same steps for transmission probabilities using the corresponding equations from Section 3.2.

4.1 Data generation

We simulate data from the model in (1) under three different scenarios. In Setting 1, we assume that there is no unmeasured correlation in the model by setting $\theta_i = 0$ for all i . This represents the most common assumption made by existing work in this area. In Setting 2, we simulate data exactly from the model in (1). In Setting 3, we simulate data from a model that is misspecified with respect to our newly introduced model such that

$$\ln(Y_{ij}) = \mathbf{x}_{ij}^T \boldsymbol{\beta} + (\mathbf{d}_i + \mathbf{d}_j)^T \boldsymbol{\gamma} + \theta_i + \theta_j + \theta_i^2 + \theta_j^2 + 2\theta_i\theta_j + \epsilon_{ij}; \quad (6)$$

where all terms have been previously described in Section 3.1. Due to the squared and interaction terms in (6), the resulting induced correlation may be more complicated than our new method is able to accommodate.

When simulating data from these models, we use results from our data application in the Republic of Moldova (Section 5) to ensure that we are working with realistic outcomes. Specifically, we use the same sample size ($n = 99$), same covariates (\mathbf{x}_{ij} , \mathbf{d}_i), and choose the true parameter values needed to simulate from (1) based on posterior estimates obtained from the data application. In Table S1 of the Supplementary Material, the specific values used in each simulation study are

given. Posterior means are used unless there is substantial skewness in the distribution, in which case the posterior median is used.

When simulating data from Setting 2, we generate a new vector of spatially correlated $\boldsymbol{\eta}$ parameters for each dataset from the prior model in (2). We then use $\boldsymbol{\eta}$ to generate $\boldsymbol{\theta}$, also from its prior model in (2), and center the $\boldsymbol{\theta}$ vector by subtracting off its mean value. This allows the specific correlation/transmission pattern of risk to change with each dataset so that we can investigate the model performances across a wide range of behaviors. For Setting 3, we simulate $\boldsymbol{\theta}$ in the same way as in Setting 2 but use the more complicated model form in (6) when defining the mean of the response. In total, we simulate 100 datasets from each setting.

4.2 Competing models

We apply two competing models to every dataset and compare the results to determine (i) the impact of ignoring correlation on regression parameter inference, (ii) if our new method can correct for this issue when the correlation is correctly specified, and (iii) if our method can perform well when it is misspecified with respect to the true data generating model. The first model represents a simplification of (1) where $\theta_i = 0$ for all i . As this model matches the data generated from Setting 1, we expect it to perform well overall in that setting. However, in Settings 2 and 3, this model will likely struggle in estimating the associations of interest as it ignores the correlation. The other competing model is our newly developed model in Section 3.1. As this model matches the data generation form of Setting 2, we hypothesize that it will perform well in that setting. However, in Setting 3, it is currently unclear how the model will perform given that the random effect parameter structure is misspecified.

We monitor a few different pieces of information collected from the simulation study to compare the two methods. First, we calculate the mean absolute error (MAE) for every regression parameter in the model using the posterior mean as the point estimate. Next, we calculate 95% quantile-based equal-tailed credible intervals (CIs) for each regression parameter and monitor how often this

interval includes the true value (ideally around 95% of the time) and its length. Finally, we formally compare the models using Watanabe Akaike information criterion (WAIC), a metric that balances model fit and complexity where smaller values suggest that a model is preferred (Watanabe, 2010). If WAIC proves to be a useful tool, it will find very little difference between the two methods in Setting 1 but begin to favor the new method as the data generating model increases in complexity (i.e., Settings 2 and 3). This would suggest that WAIC can identify which setting a researcher is in with their own data, and could inform about which model may be preferred in future applications.

4.3 Results

We apply each method to each dataset and collect 20,000 posterior samples after removing the first 5,000 iterations prior to convergence of the model. Additionally, we thin the remaining samples by a factor of two to reduce posterior autocorrelation, resulting in 10,000 samples for making posterior inference. The priors from Sections 3.1.1 and 3.2.1 were used other than when the full transmission probability model from Section 3.2 was applied to data generated from Setting 1. In that case $\phi \sim \text{Gamma}(10.00, 10.00)$ was used to stabilize estimation of that parameter. The results are shown in Table 2 for both models where we report the average MAE, average empirical coverage (EC), and average CI length across all regression parameters and simulated datasets, as well as the average difference in WAIC values across all simulated datasets (standard minus new).

In Setting 1, as expected the standard methods that ignores correlation are slightly preferred with respect to MAE and EC, though our new methods provides very similar values overall. WAIC also correctly selects the most appropriate model on average in this setting. However, in Settings 2 and 3 where correlation is present, the new methods greatly outperform the standard methods across all metrics. The standard methods display troubling behavior in these settings, particularly with respect to EC. The 95% CIs are only capturing the true parameter values around 41-60% of the times as they are much shorter on average than those from the new methods. This suggests that failing to account for correlation may result in CIs that are too narrow, possibly leading to

Table 2: Simulation study results. $\Delta \text{WAIC} = \text{WAIC}_{\text{standard}} - \text{WAIC}_{\text{new}}$. Averages across the 100 simulated datasets are reported with standard errors given in parentheses. Bold entries indicate the “best” value within a setting and outcome type across models. MAE results are multiplied by 100 for presentation purposes.

Metric	Setting	Patristic		Trans. Probs.	
		Standard	New	Standard	New
MAE	1	1.06 (0.03)	1.08 (0.04)	6.34 (0.13)	6.42 (0.13)
	2	5.54 (0.18)	4.97 (0.18)	13.79 (0.28)	12.14 (0.23)
	3	6.12 (0.21)	5.65 (0.21)	15.44 (0.38)	12.76 (0.26)
EC	1	0.94 (0.01)	0.98 (0.00)	0.95 (0.00)	0.97 (0.00)
	2	0.42 (0.01)	0.94 (0.01)	0.60 (0.01)	0.91 (0.01)
	3	0.41 (0.02)	0.93 (0.01)	0.53 (0.01)	0.90 (0.01)
CI Length	1	0.05 (0.00)	0.06 (0.00)	0.31 (0.00)	0.34 (0.00)
	2	0.08 (0.00)	0.24 (0.00)	0.31 (0.00)	0.52 (0.00)
	3	0.09 (0.00)	0.26 (0.00)	0.29 (0.00)	0.52 (0.00)
ΔWAIC	1	-29.65 (0.97)		-32.33 (0.96)	
	2	4917.35 (48.38)		2532.44 (45.88)	
	3	4632.57 (47.20)		2302.58 (31.03)	

an inflated type I error rate. The MAE results suggest that the point estimates may also suffer when correlation is ignored, though the differences are less extreme. The WAIC results in Settings 2 and 3 are decisively in favor of the new methods. When combined with results from Setting 1, this provides evidence that WAIC may be a useful tool for differentiating datasets in terms of correlation.

Overall, the new methods continue to produce valid statistical inference for the regression parameters of interest under more complicated, and misspecified, data generating scenarios, while never being meaningfully outperformed in the simpler setting. This suggests that they should

be used regardless of setting, though WAIC may be helpful in determining the need for the new methods if a user is deciding between them and the standard approaches.

5 Data application

We apply the methods developed in Sections 3.1 and 3.2 to better understand factors related to *Mycobacterium tuberculosis* transmission dynamics in the Republic of Moldova. Specifically, \mathbf{x}_{ij} from (1, 4, 5) includes the paired covariates described in Section 2 and Table 1 (i.e., intercept, same village indicator, distance between villages, difference in diagnosis dates, difference in ages) while \mathbf{d}_i includes the individual covariates (i.e., age, sex, education, working status, residence type). In addition to the new methods, we also present results from the more standard approaches detailed in Section 4.2. Briefly, the standard approaches ignore all correlation in the data and are nested within the new methods such that in (1) $\theta_i = 0$ for all i and in (4,5) $\theta_{zi}^{(g)} = \theta_{zi}^{(r)} = \theta_{wi}^{(g)} = \theta_{wi}^{(r)} = 0$ for all i . We use WAIC to compare the different models and determine the need for the new methodology.

All models are fit in the Bayesian setting using MCMC sampling techniques, with the full conditional distributions detailed in Section S1 of the Supplementary Material. For each method, we collect 10,000 samples from the joint posterior distribution after removing the first 50,000 iterations prior to convergence and thinning the remaining 200,000 posterior samples by a factor of 20 to reduce posterior autocorrelation. For each parameter, convergence was assessed using Geweke’s diagnostic (Geweke, 1991) while effective sample size was calculated to ensure we collected sufficient post-convergence samples to make accurate statistical inference. Neither tool suggested any issues of concern. We present posterior means and 95% quantile-based equal-tailed CIs when discussing posterior inference.

5.1 Patristic distances

The results from the patristic distance analyses are shown in Tables 3, 4, and Figure 2, where it is clear that WAIC strongly favors the newly developed method over the standard approach. In the simulation study, WAIC was shown to consistently identify the correct data generating setting, suggesting that there is non-negligible correlation in these data. Consequently, the standard approach should not be used as it is likely to underestimate regression parameter uncertainty, resulting in CIs that are often too narrow. This can be seen in Figure 2 where the standard approach identifies many more significant associations than the new method, potentially increasing the type I error rate. The point estimates seen in Figure 2 are generally consistent across both methods as expected based on the simulation study results, even in the presence of correlated data.

Posterior inference for the exponentiated regression parameters in Table 3 suggest that the indicator of whether the pair of individuals was in the same village is the only association whose CI excludes one (i.e., significant) using the new method. Patristic distances from pairs of individuals from the same village are around 45% (40%, 49%) smaller on average than those from pairs individuals in different villages.

Table 4 displays various summaries of the estimated random effect parameters. We observe that 57 of the 99 parameters have CIs that exclude zero; 29 of which are positive and 28 that are negative. Recall that individuals with positive θ_i are more likely to be in pairs with larger patristic distances (i.e., less likely transmission) while those with negative θ_i are more likely to be in pairs with small patristic distances (i.e., transmission pair). To test this, we calculate the average patristic distance for all outcome pairs that involve the individuals with significantly positive θ_i , and repeat the calculation for those with significantly negative θ_i . For reference, the average patristic distance overall (multiplied by 10,000 for presentation purposes) is 3.12 while for the positive and negative random effect parameter pairs is 3.96 and 2.47, respectively. This shows the intuitive connection between the raw data and estimated values of these parameters. The total variability in the θ_i parameters is largely driven by individual behavior rather than spatial correlation/clustering as

Table 3: Results from the patristic distance analyses in the Republic of Moldova. Posterior means and 95% quantile-based equal-tailed credible intervals are shown for the exponentiated regression parameters (i.e., relative risk). The displayed credible intervals for the bolded entries exclude one.

Effect	Standard (WAIC: 4,515.93)	New (WAIC: -133.23)
Distance Between Villages (50 km)	0.98 (0.97, 0.99)	1.00 (0.99, 1.01)
Same Village (Yes vs. No)	0.59 (0.52, 0.67)	0.55 (0.51, 0.60)
Date of Diagnosis Difference (1/2 Year)	1.03 (1.02, 1.04)	1.01 (1.00, 1.01)
Age Difference (10 Years)	1.01 (1.01, 1.02)	1.00 (0.99, 1.01)
Age (10 Years)	1.00 (0.99, 1.00)	1.00 (0.95, 1.04)
Sex:		
Mixed Pair vs. Both Female	0.98 (0.94, 1.03)	0.99 (0.88, 1.11)
Both Male vs. Both Female	0.98 (0.94, 1.03)	0.99 (0.78, 1.24)
Residence Location:		
Mixed Pair vs. Both Rural	0.98 (0.96, 1.00)	0.98 (0.88, 1.08)
Both Urban vs. Both Rural	0.96 (0.93, 1.00)	0.97 (0.78, 1.19)
Working Status:		
Mixed Pair vs. Both Unemployed	0.98 (0.95, 1.00)	0.98 (0.84, 1.14)
Both Employed vs. Both Unemployed	0.98 (0.87, 1.09)	1.00 (0.72, 1.35)
Education:		
Mixed Pair vs. Both \geq Secondary	1.05 (1.03, 1.08)	1.05 (0.95, 1.17)
Both $<$ Secondary vs. Both \geq Secondary	1.11 (1.07, 1.15)	1.12 (0.90, 1.37)

seen when analyzing the posterior distribution of $\tau^2 / (\tau^2 + \sigma_\zeta^2)$ (0.23; 0.05-0.68).

In Figures S1 and S2 of the Supplement, we display posterior means and standard deviations, respectively, for the random effect parameters predicted across the Republic of Moldova. To produce these maps, we create an equally spaced grid over the domain containing 500 new locations (i.e., where data were not previously observed) and then collect samples from the posterior predic-

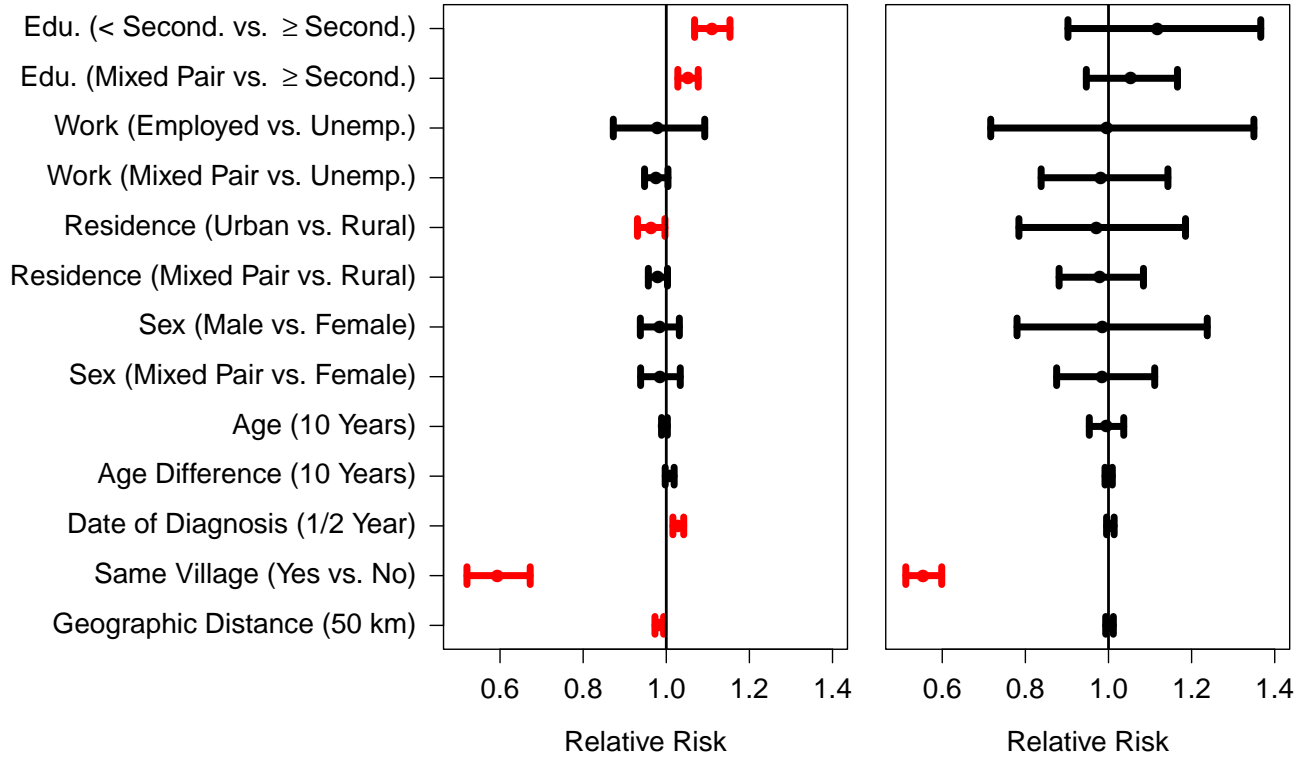


Figure 2: Results from the patristic distance analyses in the Republic of Moldova. Posterior means and 95% quantile-based equal-tailed credible intervals are shown for the exponentiated regression parameters from the standard model (left panel) and new method (right panel). Red lines indicate that the interval excludes one.

tive distribution for the random effect parameters at each location separately (i.e., samples from $f\{\theta_0 | \ln(Y_{12}), \dots, \ln(Y_{n-1,n})\}$). These samples are then summarized using posterior means and standard deviations and plotted across the domain using inverse distance weighting to fill in the remaining gaps (for visualization purposes only). Areas in red from the posterior mean map suggest that patristic distances involving individuals residing in these locations tend to be smaller on

Table 4: Random effect parameter results from all analyses in the Republic of Moldova. The table presents the number of parameters with 95% quantile-based equal-tailed credible intervals (CIs) that exclude zero (positive and negative), summaries of the outcome variables (i.e., patristic distances and transmission probabilities (TP)) overall and for each significance group, and the proportion of total variability in the parameters that is spatially structured.

Model	# of Significant θ_i		Outcome Summary ¹			Spatial Variability ²
	> 0	< 0	Overall	$\theta_i > 0$	$\theta_i < 0$	
Patristic	29	28	3.12	3.96	2.47	0.23 (0.05, 0.68)
TP: Binary, Giver	29	22	71.72	54.73	87.20	0.50 (0.29, 0.69)
TP: Binary, Receiver	29	24	71.72	54.52	87.35	0.47 (0.26, 0.66)
TP: Continuous, Giver	6	13	0.86	1.40	0.89	0.91 (0.74, 0.99)
TP: Continuous, Receiver	16	18	0.86	1.15	1.32	0.94 (0.82, 0.99)

¹ Patristic: Average patristic distance multiplied by 10,000; TP: Binary: Percentage of transmission probabilities equal to zero; TP: Continuous: Average of the positive transmission probabilities multiplied by 100.

² Patristic: Posterior mean and 95% CI of $\tau^2/(\tau^2 + \sigma_\zeta^2)$; TP: Binary, Giver: Posterior mean and 95% CI for $\omega_{11}/(\omega_{11} + \sigma_{\zeta_z(g)}^2)$ where ω_{11} is the (1, 1) entry of Ω ; similar definitions for TP: Binary, Receiver; TP: Continuous, Giver; and TP: Continuous, Receiver.

average than areas in blue, possibly indicating geographic areas of increased residual transmission activity. However, the variability in these values overall is not large in this setting, suggesting that the risk does not differ substantially across the map.

5.2 Transmission probabilities

Similar to the patristic distance analyses, WAIC also favors the new transmission probability method over the standard approach in this setting (WAIC_{standard}: 23,238.10; WAIC_{new}: 21,546.43).

In Table 5, we display results from the binary (4) and continuous (5) components of the model. Comparable graphical results are shown in Figure S3 of the Supplementary Material. Once again, the standard approach may be producing CIs that are too narrow, leading to several more significant associations being identified when compared to the new method (i.e., likely type I errors). In both regression models (binary and continuous), odds ratio results from the new method suggest that pairs of individuals in the same village are more likely to have non-zero transmission probabilities (4.04; 2.35, 6.60) and, given that they are non-zero, increasing magnitudes (46.70; 21.97, 88.38) on average. Additionally, pairs with similar dates of diagnosis are more likely to have non-zero (0.87; 0.81, 0.93) and increasing transmission probabilities (0.78; 0.71, 0.86) on average. Giver and receiver individual-level covariate parameter estimates are generally similar and non-significant.

In Table 4, summaries of the random effect parameters are displayed. As expected, individuals identified with significant, positive random effect parameters (both giver and receiver type) are less likely to have a zero transmission probability. The results for the continuous component of the model are mixed, likely due to the smaller number of transmission probabilities that were larger than zero (i.e., 71.72% were equal to zero). Individual role (i.e., giver/receiver)- and model component (i.e., binary/continuous)-specific maps of random effect parameter predictions and uncertainties are displayed in Figures S2 and S3 of the Supplement, with areas in red suggesting that transmission probabilities involving individuals residing in these areas are generally larger than those from individuals in the blue areas.

6 Discussion

In this work, we presented innovative hierarchical Bayesian statistical methods for correctly modeling two types of paired genetic relatedness data, patristic distances and transmission probabilities. The models account for multiple sources of correlation (i.e., paired data and spatial) and important features of each outcome (e.g., zero-inflation, non-Gaussian distribution). Through simulation we showed that these approaches perform as well as the standard approaches (i.e., regression while

Table 5: Results from the transmission probability analyses in the Republic of Moldova. Posterior means and 95% quantile-based equal-tailed credible intervals are shown for the exponentiated regression parameters (i.e., odds ratios). $WAIC_{\text{standard}}$: 23,238.10; $WAIC_{\text{new}}$: 21,546.43.

Effect	Binary		Continuous	
	Standard	New	Standard	New
Distance Between Villages (50 km)	1.15 (1.10, 1.20)	1.03 (0.97, 1.09)	0.97 (0.90, 1.04)	0.92 (0.84, 1.01)
Same Village (Yes vs. No)	3.09 (1.86, 4.82)	4.04 (2.35, 6.60)	34.71 (16.35, 65.29)	46.70 (21.97, 88.38)
Date of Diagnosis Difference (1/2 Year)	0.83 (0.79, 0.88)	0.87 (0.81, 0.93)	0.83 (0.75, 0.91)	0.78 (0.71, 0.86)
Age Difference (10 Years)	0.98 (0.94, 1.03)	1.00 (0.94, 1.06)	0.95 (0.88, 1.03)	0.92 (0.84, 1.01)
Giver Role:				
Age (10 Years)	1.02 (0.98, 1.06)	1.02 (0.92, 1.13)	1.00 (0.93, 1.07)	1.01 (0.91, 1.11)
Sex:				
Male vs. Female	1.11 (0.99, 1.24)	1.16 (0.87, 1.52)	1.15 (0.93, 1.40)	1.17 (0.89, 1.53)
Residence Location:				
Urban vs. Rural	1.01 (0.92, 1.11)	0.99 (0.77, 1.24)	1.11 (0.94, 1.30)	1.22 (0.86, 1.68)
Working Status:				
Employed vs. Unemployed	1.00 (0.85, 1.16)	1.04 (0.69, 1.50)	1.13 (0.85, 1.46)	1.09 (0.74, 1.57)
Education:				
< Secondary vs. \geq Secondary	0.99 (0.90, 1.09)	0.97 (0.75, 1.23)	1.11 (0.93, 1.31)	1.13 (0.86, 1.46)
Receiver Role:				
Age (10 Years)	1.03 (0.99, 1.07)	1.04 (0.93, 1.16)	1.01 (0.94, 1.09)	1.04 (0.94, 1.16)
Sex:				
Male vs. Female	1.06 (0.95, 1.19)	1.12 (0.81, 1.52)	1.31 (1.07, 1.59)	1.27 (0.93, 1.68)
Residence Location:				
Urban vs. Rural	0.97 (0.88, 1.07)	0.94 (0.71, 1.21)	1.23 (1.04, 1.44)	1.39 (0.94, 2.01)
Working Status:				
Employed vs. Unemployed	0.95 (0.82, 1.11)	0.99 (0.62, 1.49)	1.32 (1.00, 1.72)	1.20 (0.77, 1.80)
Education:				
< Secondary vs. \geq Secondary	1.02 (0.92, 1.12)	1.00 (0.75, 1.32)	1.13 (0.94, 1.33)	1.13 (0.84, 1.50)

ignoring correlation) when applied to uncorrelated data, and greatly outperform them under correlation in terms of estimating and quantifying uncertainty in the regression parameters. Notably, the model was shown to be robust to a more complex misspecified correlation structure, still producing valid inference for the regression parameters of interest. Under any level of correlation, the standard approach produces CIs that are too narrow and as a result should not be used for estimating associations between genetic relatedness measures and other factors. When applying the models to *Mycobacterium tuberculosis* data from the Republic of Moldova, we found significant associations between genetic relatedness and spatial proximity, as well as dates of diagnosis. Analysis of the random effect parameters identified individuals and geographic areas that are generally associated with higher levels of transmission, a potentially useful aspect of the model with respect to infection control. Heterogeneity in infectiousness among TB patients has been investigated in previous studies (Ypma et al., 2013; Melsew et al., 2019).

The unique data in our study represent a major strength of the work, however, a number of factors inherent to *Mycobacterium tuberculosis* make the study of transmission dynamics difficult. First, TB epidemics are relatively slow moving, often occurring over years (Pai et al., 2016), and it is difficult to observe these processes in a two-year study. Second, the time between infection and disease onset varies greatly, from weeks to years (Borgdorff et al., 2011). Third, not all TB cases are ‘culture positive’, meaning it is more difficult to culture, and, by extension, sequence isolates for every known TB case (Cruciani et al., 2004; Nguyen et al., 2019). Taken together, these factors make it difficult to infer direct transmission events. Even within a putative transmission cluster, the probabilities of direct transmission among case pairs may be low. For this reason, it can be difficult to fit a model to these types of data. We address this challenge by including a binary component in our model specification (i.e., an indicator of a non-zero transmission probability between case pairs). Finally, as is standard in most epidemiological analyses, our data do not include information on individuals who were exposed but not infected. Therefore, the results should be interpreted conditional on both individuals being infected.

While we use patristic distance as an outcome representative of symmetric paired genetic relatedness data in this work, the framework we’ve created can be readily adapted to SNP distances by modifying the likelihood in (1) to accommodate discrete count data (e.g., Poisson, negative binomial). Future work in this area could focus on alternative techniques for accounting for the

correlation caused by analyzing paired outcomes. Our current methods are based on the idea of shared random effect parameters between pairs of data including the same individual, which was shown to induce an intuitive correlation structure between observations in Section 3.3. Additionally, these parameters were shown to be useful in identifying key individuals/areas that drive transmission in the study. However, there are likely other approaches for achieving these goals.

Overall, we recommend the use of the newly developed methods when the goal of a study is to estimate associations between genetic relatedness and other variables of interest. Both methods are available in our R package **GenePair** (available at: <https://github.com/warrenjl/GenePair>). Even under the most simplistic, and likely unrealistic assumption of no correlation between paired responses, the new methodology performs well. When correlation is present, the standard approaches often used in practice yield potentially overly optimistic insights about the significance of the associations and should not be used for decision making.

References

- Alberto, F., L. Gouveia, S. Arnaud-Haond, J. L. Perez-Llorens, C. M. Duarte, and E. A. Serrao (2005). Within-population spatial genetic structure, neighbourhood size and clonal subrange in the seagrass *Cymodocea nodosa*. *Molecular Ecology* 14(9), 2669–2681.
- Balaban, M., N. Moshiri, U. Mai, X. Jia, and S. Mirarab (2019, 08). Treecluster: Clustering biological sequences using phylogenetic trees. *PLoS ONE* 14(8), 1–20.
- Borgdorff, M. W., M. Sebek, R. B. Gesskus, K. Kremer, N. Kalisvaart, and D. van Soolingen (2011). The incubation period distribution of tuberculosis estimated with a molecular epidemiological approach. *International Journal of Epidemiology* 40(4), 964–970.
- Campbell, F., A. Cori, N. Ferguson, and T. Jombart (2019, 03). Bayesian inference of transmission

- chains using timing of symptoms, pathogen genomes and contact data. *PLoS Computational Biology* 15, 1–20.
- Cruciani, M., C. Scarparo, M. Malena, O. Bosco, G. Serpelloni, and C. Mengoli (2004). Meta-analysis of BACTEC MGIT 960 and BACTEC 460 TB, with or without solid media, for detection of mycobacteria. *Journal of Clinical Microbiology* 42(5), 2321–2325.
- Delsuc, F., H. Brinkmann, and H. Philippe (2005). Phylogenomics and the reconstruction of the tree of life. *Nature Review Genetics* 6, 361–375.
- Didelot, X., C. Fraser, J. Gardy, and C. Colijn (2017). Genomic infectious disease epidemiology in partially sampled and ongoing outbreaks. *Molecular Biology and Evolution* 34(4), 997–1007.
- Gates, E. D. H., J. Yang, K. Fukumura, J. S. Lin, J. S. Weinberg, S. S. Prabhu, L. Long, D. Fuentes, E. P. Sulman, J. T. Huse, and D. Schellingerhout (2019). Spatial distance correlates with genetic distance in diffuse glioma. *Frontiers in Oncology* 9, 676.
- Gelman, A., J. B. Carlin, H. S. Stern, D. B. Dunson, A. Vehtari, and D. B. Rubin (2013). *Bayesian Data Analysis*. CRC press.
- Geweke, J. (1991). *Evaluating the Accuracy of Sampling-based Approaches to the Calculation of Posterior Moments*, Volume 196. Federal Reserve Bank of Minneapolis, Research Department Minneapolis, MN, USA.
- Kitchen, A. M., E. M. Geese, L. P. Waits, S. M. Karki, and E. R. Schauster (2005). Genetic and spatial structure within a swift fox population. *Journal of Animal Ecology* 74, 1173–1181.
- Klinkenberg, D., J. A. Backer, X. Didelot, C. Colijn, and J. Wallinga (2017, 05). Simultaneous inference of phylogenetic and transmission trees in infectious disease outbreaks. *PLoS Computational Biology* 13, 1–32.

- Lieberman, T., D. Wilson, R. Misra, L. Xiong, P. Moodley, T. Cohen, and R. Kosony (2016). Genomic diversity in autopsy samples reveals within-host dissemination of HIV-associated Mycobacterium tuberculosis. *Nature Medicine* 22, 1470–1474.
- Loman, N. and M. Pallen (2015). Twenty years of bacterial genome sequencing. *Nature Review Microbiology* 13, 787–794.
- Melsew, Y. A., M. Gambhir, A. C. Cheng, E. S. McBryde, J. T. Denholm, E. L. Tay, and J. M. Trauer (2019). The role of super-spreading events in Mycobacterium tuberculosis transmission: evidence from contact tracing. *BMC Infectious Diseases* 19(1), 1–9.
- Nguyen, M.-V. H., N. S. Levy, S. D. Ahuja, L. Trieu, D. C. Proops, and J. M. Achkar (2019, 02). Factors associated with sputum culture-negative vs culture-positive diagnosis of pulmonary tuberculosis. *JAMA Network Open* 2(2), e187617–e187617.
- Omedo, I., P. Mogeni, T. Bousema, K. Rockett, A. Amambua-Ngwa, I. Oyier, J. Stevenson, A. Baidjoe, E. de Villiers, G. Fegan, A. Ross, C. Hubbart, A. Jeffreys, T. Williams, D. Kwiatkowski, and P. Bejon (2017). Micro-epidemiological structuring of Plasmodium falciparum parasite populations in regions with varying transmission intensities in Africa. *Wellcome Open Research* 2(10).
- Pai, M., M. A. Behr, D. Dowdy, K. Dheda, M. Divangahi, C. C. Boehme, A. Ginsberg, S. Swaminathan, M. Spigelman, H. Getahun, D. Menzies, and M. Raviglione (2016). Tuberculosis. *Nature Reviews Disease Primers* 2(1), 16076.
- Polonsky, J. A., A. Baidjoe, Z. N. Kamvar, A. Cori, K. Durski, W. J. Edmunds, R. M. Eggo, S. Funk, L. Kaiser, P. Keating, et al. (2019). Outbreak analytics: a developing data science for informing the response to emerging pathogens. *Philosophical Transactions of the Royal Society B* 374(1776), 20180276.

- Poon, A. F. Y. (2016). Impacts and shortcomings of genetic clustering methods for infectious disease outbreaks. *Virus Evolution* 2(2). vew031.
- Stamatakis, A. (2014, 01). RAxML version 8: a tool for phylogenetic analysis and post-analysis of large phylogenies. *Bioinformatics* 30(9), 1312–1313.
- Sy, M., A. B. Deme, J. L. Warren, R. F. Daniels, B. Dieye, P. I. Ndiaye, Y. Diedhiou, A. M. Mbaye, S. K. Volkman, D. L. Hartl, D. F. Wirth, D. Ndiaye, and A. K. Bei (2020). *Plasmodium falciparum* genomic surveillance reveals spatial and temporal trends, association of genetic and physical distance, and household clustering. *medRxiv*, 2020.12.24.20248574.
- Vekemans, X. and O. Hardy (2004). New insights from fine-scale spatial genetic structure analyses in plant populations. *Molecular Ecology* 13, 921–935.
- Walker, T. M., M. K. Lalor, A. Broda, L. S. Ortega, M. Morgan, L. Parker, S. Churchill, K. Bennett, T. Golubchik, A. P. Giess, C. Del Ojo Elias, K. J. Jeffery, I. C. J. W. Bowler, I. F. Laurenson, A. Barrett, F. Drobniewski, N. D. McCarthy, L. F. Anderson, I. Abubakar, H. L. Thomas, P. Monk, E. G. Smith, A. S. Walker, D. W. Crook, T. E. A. Peto, and C. P. Conlon (2014). Assessment of Mycobacterium tuberculosis transmission in Oxfordshire, UK, 2007–12, with whole pathogen genome sequences: an observational study. *The Lancet Respiratory Medicine* 2(4), 285–292.
- Watanabe, S. (2010). Asymptotic equivalence of Bayes cross validation and widely applicable information criterion in singular learning theory. *Journal of Machine Learning Research* 11, 3571–3594.
- Yang, C., B. Sobkowiak, V. Naidu, A. Codreanu, N. Ciobanu, K. S. Gunasekera, M. H. Chitwood, S. Alexandru, S. Bivol, M. Russi, J. Havumaki, P. Cudahy, H. Fosburgh, C. J. Allender, H. Centner, D. M. Engelthaler, N. A. Menzies, J. L. Warren, V. Crudu, C. Colijn, and T. Cohen (2021). Phylogeography and transmission of M. tuberculosis in Moldova. *medRxiv*, 2021.06.30.21259748.

Ypma, R. J., H. K. Altes, D. Van Soolingen, J. Wallinga, and W. M. Van Ballegooijen (2013).
A sign of superspreading in tuberculosis: highly skewed distribution of genotypic cluster sizes.
Epidemiology 24(3), 395–400.

Supplementary Material for “Statistical methods for analyzing spatially-referenced paired genetic relatedness data”

Joshua L. Warren¹, Melanie H. Chitwood², Benjamin Sobkowiak³,
Valeriu Crudu⁴, Caroline Colijn³, Ted Cohen²

¹Department of Biostatistics, Yale University, New Haven, CT 06510, USA

²Department of Epidemiology of Microbial Diseases, Yale University, New Haven, CT 06510, USA

³Department of Mathematics, Simon Fraser University, Burnaby, BC V5A 1S6, CA

⁴Microbiology and Morphology Laboratory, Phthisiopneumology Institute, Chisinau, MLD
(E-mail: joshua.warren@yale.edu)

S1 Model fitting details

We use Markov chain Monte Carlo sampling techniques (i.e., Gibbs and Metropolis-within-Gibbs algorithms) to fit the newly developed models within our R package **GenePair** (available at: <https://github.com/warrenjl/GenePair>) (Metropolis et al., 1953; Geman and Geman, 1984; Gelfand and Smith, 1990). In this section we present the full conditional distributions for all introduced model parameters needed to fit both of the models (i.e., patristic distances and transmission probabilities).

S1.1 Patristic distances

The patristic distances model in Section 3.1 of the main text can be written more generally in the linear mixed model format such as

$$\mathbf{Y} = X\boldsymbol{\delta} + Z\boldsymbol{\theta} + \boldsymbol{\epsilon}$$

where $\boldsymbol{\epsilon}|\sigma_\epsilon^2 \sim \text{MVN}(\mathbf{0}_{n^*}, \sigma_\epsilon^2 I_{n^*})$; $n^* = \sum_{i=1}^{n-1} \sum_{j=i+1}^n 1$ is the total number of unique-pair patristic distances in the study; n is the number of individuals in the study; I_{n^*} is the n^* by n^* identity matrix; $\mathbf{Y}^T = \{\ln(Y_{12}), \dots, \ln(Y_{n-1,n})\}$ is the full vector of log-scaled patristic distances (i.e., $\ln(Y_{ij})$, $i \neq j$, $i < j$); X is an n^* by $(p_x + p_d)$ matrix of covariates with i^{th} row (corresponding to pair (j, k) of data for example) equal to $\{\mathbf{x}_{jk}^T, (\mathbf{d}_j + \mathbf{d}_k)^T\}$; $\boldsymbol{\delta}^T = (\boldsymbol{\beta}^T, \boldsymbol{\gamma}^T)$; Z is an n^* by n matrix with i^{th} row (corresponding to pair (j, k) of data for example) equal to a vector of all zeros other than entries j and k which are equal to one; and $\boldsymbol{\theta}^T = (\theta_1, \dots, \theta_n)$.

The prior distributions match those from Section 3.1.1 of the main text with $\boldsymbol{\delta} \sim \text{MVN}(\mathbf{0}_{(p_x+p_d)}, 100^2 I_{(p_x+p_d)})$ and $\mathbf{0}_p$ is a p -length vector of zeros; $\boldsymbol{\theta}|\boldsymbol{\eta}, \sigma_\zeta^2 \sim \text{MVN}(V\boldsymbol{\eta}, \sigma_\zeta^2 I_n)$ where V is an n by m matrix with $V_{ij} = 1$ if individual i resides at location \mathbf{s}_j^* and

$V_{ij} = 0$ otherwise; $\boldsymbol{\eta}|\phi, \tau^2 \sim \text{MVN}\{\mathbf{0}_m, \tau^2 \Sigma(\phi)\}$; $\phi \sim \text{Gamma}(1.00, 1.00)$; and $\sigma_\epsilon^2, \sigma_\zeta^2, \tau^2 \stackrel{\text{iid}}{\sim} \text{Inverse Gamma}(0.01, 0.01)$. For complete details on the definitions for each of these variables/parameters, please see Section 3.1 of the main text.

Based on these specifications, the full conditional distributions are given as:

- $\sigma_\epsilon^2 | \Theta_{-\sigma_\epsilon^2}, \mathbf{Y} \sim \text{Inverse Gamma}\left(\frac{n^*}{2} + 0.01, \frac{(\mathbf{Y} - \mathbf{X}\boldsymbol{\delta} - \mathbf{Z}\boldsymbol{\theta})^\text{T}(\mathbf{Y} - \mathbf{X}\boldsymbol{\delta} - \mathbf{Z}\boldsymbol{\theta})}{2} + 0.01\right)$, where $\Theta_{-\sigma_\epsilon^2}$ is the full vector of all parameters with σ_ϵ^2 removed;
- $\boldsymbol{\delta} | \Theta_{-\boldsymbol{\delta}}, \mathbf{Y} \sim \text{MVN}(\Sigma_{\boldsymbol{\delta}}, \boldsymbol{\mu}_{\boldsymbol{\delta}})$ with $\Sigma_{\boldsymbol{\delta}} = \left(\frac{\mathbf{X}^\text{T}\mathbf{X}}{\sigma_\epsilon^2} + \frac{I_{(p_x+p_d)}}{100^2}\right)^{-1}$ and $\boldsymbol{\mu}_{\boldsymbol{\delta}} = \frac{\Sigma_{\boldsymbol{\delta}}\mathbf{X}^\text{T}(\mathbf{Y} - \mathbf{Z}\boldsymbol{\theta})}{\sigma_\epsilon^2}$;
- $\boldsymbol{\theta} | \Theta_{-\boldsymbol{\theta}}, \mathbf{Y} \sim \text{MVN}(\Sigma_{\boldsymbol{\theta}}, \boldsymbol{\mu}_{\boldsymbol{\theta}})$ with $\Sigma_{\boldsymbol{\theta}} = \left(\frac{\mathbf{Z}^\text{T}\mathbf{Z}}{\sigma_\epsilon^2} + \frac{I_n}{\sigma_\zeta^2}\right)^{-1}$ and $\boldsymbol{\mu}_{\boldsymbol{\theta}} = \Sigma_{\boldsymbol{\theta}} \left\{ \frac{\mathbf{Z}^\text{T}(\mathbf{Y} - \mathbf{X}\boldsymbol{\delta})}{\sigma_\epsilon^2} + \frac{\mathbf{V}\boldsymbol{\eta}}{\sigma_\zeta^2} \right\}$; we implement a sum-to-zero constraint *on the fly* for these parameters (Besag et al., 1995; Berrocal et al., 2012; Warren et al., 2021);
- $\sigma_\zeta^2 | \Theta_{-\sigma_\zeta^2}, \mathbf{Y} \sim \text{Inverse Gamma}\left(\frac{n}{2} + 0.01, \frac{(\boldsymbol{\theta} - \mathbf{V}\boldsymbol{\eta})^\text{T}(\boldsymbol{\theta} - \mathbf{V}\boldsymbol{\eta})}{2} + 0.01\right)$;
- $\boldsymbol{\eta} | \Theta_{-\boldsymbol{\eta}}, \mathbf{Y} \sim \text{MVN}(\Sigma_{\boldsymbol{\eta}}, \boldsymbol{\mu}_{\boldsymbol{\eta}})$ with $\Sigma_{\boldsymbol{\eta}} = \left(\frac{\mathbf{V}^\text{T}\mathbf{V}}{\sigma_\zeta^2} + \frac{\Sigma(\phi)^{-1}}{\tau^2}\right)^{-1}$ and $\boldsymbol{\mu}_{\boldsymbol{\eta}} = \frac{\Sigma_{\boldsymbol{\eta}}\mathbf{V}^\text{T}\boldsymbol{\theta}}{\sigma_\zeta^2}$;
- $\tau^2 | \Theta_{-\tau^2}, \mathbf{Y} \sim \text{Inverse Gamma}\left(\frac{m}{2} + 0.01, \frac{\boldsymbol{\eta}^\text{T}\Sigma(\phi)^{-1}\boldsymbol{\eta}}{2} + 0.01\right)$; and
- $f\{\ln(\phi) | \text{rest}\} \propto |\Sigma(\phi)^{-1}|^{1/2} \exp\left\{-\frac{1}{2\tau^2}\boldsymbol{\eta}^\text{T}\Sigma(\phi)^{-1}\boldsymbol{\eta}\right\} f\{\ln(\phi)\}$; during model fitting, we work with $\ln(\phi) \in \mathbb{R}$ instead of ϕ so that a symmetric proposal density can be used in the Metropolis algorithm.

S1.2 Transmission probabilities

From the transmission probabilities model introduced in Section 3.2 of the main text, we work with the complete vector of observed transmission probabilities, \mathbf{Y} , whose length is $n^* = \sum_{i=1}^n \sum_{j=1, i \neq j}^n 1$ (i.e., Y_{ij} and Y_{ji} included for $i \neq j$). We also introduce a vector of latent probabilities controlling whether the transmission probabilities are > 0 (i.e., $\boldsymbol{\pi}$) and a vector of latent continuous variables representing the logit-scaled > 0 transmission probabilities

(i.e., \mathbf{w}), both of which are the same length and ordered in the same way as \mathbf{Y} . We note that not every $Y_{ij} > 0$, meaning that not every w_{ij} is directly observed. When $Y_{ij} = 0$, the corresponding w_{ij} is treated as a missing variable within this framework.

We then use the regression frameworks defined in Section 3.2 of the main text to define these latent parameter vectors such that

$$\begin{aligned}\text{logit}(\boldsymbol{\pi}) &= X\boldsymbol{\delta}_z + Z^{(g)}\boldsymbol{\theta}_z^{(g)} + Z^{(r)}\boldsymbol{\theta}_z^{(r)} \text{ and} \\ \mathbf{w} &= X\boldsymbol{\delta}_w + Z^{(g)}\boldsymbol{\theta}_w^{(g)} + Z^{(r)}\boldsymbol{\theta}_w^{(r)} + \boldsymbol{\epsilon}\end{aligned}$$

where $\boldsymbol{\epsilon}|\sigma_\epsilon^2 \sim \text{MVN}(\mathbf{0}_{n^*}, \sigma_\epsilon^2 I_{n^*})$; X is an n^* by $(p_x + 2p_d)$ matrix of covariates with i^{th} row (corresponding to pair (j, k) of data for example) equal to $\{\mathbf{x}_{jk}^T, \mathbf{d}_k^T, \mathbf{d}_j^T\}$; $\boldsymbol{\delta}_z^T = (\boldsymbol{\beta}_z^T, \boldsymbol{\gamma}_z^{(g)T}, \boldsymbol{\gamma}_z^{(r)T})$ with $\boldsymbol{\delta}_w$ defined similarly; $Z^{(g)}$ is an n^* by n matrix with i^{th} row (corresponding to pair (j, k) of data for example) equal to a vector of all zeros other than entry k which is equal to one; $Z^{(r)}$ is defined similarly to $Z^{(g)}$ where entry j is equal to one instead of entry k ; and $\boldsymbol{\theta}_z^{(g)T} = (\theta_{z1}^{(g)}, \dots, \theta_{zn}^{(g)})$ with $\boldsymbol{\theta}_z^{(r)}$, $\boldsymbol{\theta}_w^{(g)}$, and $\boldsymbol{\theta}_w^{(r)}$ defined similarly.

The prior distributions match those from Section 3.2.1 of the main text with $\boldsymbol{\delta}_z, \boldsymbol{\delta}_w \stackrel{\text{iid}}{\sim} \text{MVN}(\mathbf{0}_{(p_x+2p_d)}, 100^2 I_{(p_x+2p_d)})$; $\boldsymbol{\theta}_z^{(g)}|\boldsymbol{\eta}_z^{(g)}, \sigma_{\zeta_z^{(g)}}^2 \sim \text{MVN}(V\boldsymbol{\eta}_z^{(g)}, \sigma_{\zeta_z^{(g)}}^2 I_n)$ where $\boldsymbol{\theta}_z^{(r)}$, $\boldsymbol{\theta}_w^{(g)}$, and $\boldsymbol{\theta}_w^{(r)}$ are defined similarly; $\sigma_\epsilon^2, \sigma_{\zeta_z^{(g)}}^2, \sigma_{\zeta_z^{(r)}}^2, \sigma_{\zeta_w^{(g)}}^2, \sigma_{\zeta_w^{(r)}}^2 \stackrel{\text{iid}}{\sim} \text{Inverse Gamma}(0.01, 0.01)$; $(\boldsymbol{\eta}_z^{(g)T}, \boldsymbol{\eta}_z^{(r)T}, \boldsymbol{\eta}_w^{(g)T}, \boldsymbol{\eta}_w^{(r)T})^T | \phi, \Omega \sim \text{MVN}\{\mathbf{0}_{4m}, \Omega \otimes \Sigma(\phi)\}$; $\phi \sim \text{Gamma}(1.00, 1.00)$; and $\Sigma^{-1} \sim \text{Wishart}(5, I_4)$. For complete details on the definitions for each of these variables/parameters, please see Section 3.2 of the main text.

Because we are working in a logistic regression framework, we use the Pólya-Gamma latent variable approach for posterior sampling developed by Polson et al. (2013). Specifically, for each Y_{ij} outcome, we introduce a corresponding Pólya-Gamma distributed latent variable

such that

$$\omega_{ij}^* | \boldsymbol{\delta}_z, \theta_{zj}^{(g)}, \theta_{zi}^{(r)} \stackrel{\text{ind}}{\sim} \text{Pólya-Gamma} \left(1, \mathbf{x}_{ij}^T \boldsymbol{\beta}_z + \mathbf{d}_j^T \boldsymbol{\gamma}_z^{(g)} + \mathbf{d}_i^T \boldsymbol{\gamma}_z^{(r)} + \theta_{zj}^{(g)} + \theta_{zi}^{(r)} \right).$$

These latent variables allow for closed form full conditional distributions for several of the parameter sets and we sample from their distribution using the `pgdraw` package in R (Makalic and Schmidt, 2021).

Based on these specifications, the full conditional distributions are given as:

- $\omega_{ij}^* | \boldsymbol{\Theta}_{-\omega_{ij}^*}, \mathbf{Y} \stackrel{\text{ind}}{\sim} \text{Pólya-Gamma} \left(1, \mathbf{x}_{ij}^T \boldsymbol{\beta}_z + \mathbf{d}_j^T \boldsymbol{\gamma}_z^{(g)} + \mathbf{d}_i^T \boldsymbol{\gamma}_z^{(r)} + \theta_{zj}^{(g)} + \theta_{zi}^{(r)} \right);$
- $\boldsymbol{\delta}_z | \boldsymbol{\Theta}_{-\boldsymbol{\delta}_z}, \mathbf{Y} \sim \text{MVN}(\Sigma_{\boldsymbol{\delta}_z}, \boldsymbol{\mu}_{\boldsymbol{\delta}_z})$ with $\Sigma_{\boldsymbol{\delta}_z} = \left(X^T \Omega^* X + \frac{I_{(p_x + 2p_d)}}{100^2} \right)^{-1}$ and $\boldsymbol{\mu}_{\boldsymbol{\delta}_z} = \Sigma_{\boldsymbol{\delta}_z} X^T \Omega^* \left(\boldsymbol{\lambda} - Z^{(g)} \boldsymbol{\theta}_z^{(g)} - Z^{(r)} \boldsymbol{\theta}_z^{(r)} \right)$, where Ω^* is an n^* by n^* diagonal matrix with the diagonal vector equal to $\boldsymbol{\omega}^{*T} = (\omega_{12}^*, \dots, \omega_{n,n-1}^*)$ and $\boldsymbol{\lambda}^T = \left(\frac{1(Y_{12} > 0) - 0.50}{\omega_{12}^*}, \dots, \frac{1(Y_{n,n-1} > 0) - 0.50}{\omega_{n,n-1}^*} \right);$
- $\boldsymbol{\theta}_z^{(g)} | \boldsymbol{\Theta}_{-\boldsymbol{\theta}_z^{(g)}}, \mathbf{Y} \sim \text{MVN}(\Sigma_{\boldsymbol{\theta}_z^{(g)}}, \boldsymbol{\mu}_{\boldsymbol{\theta}_z^{(g)}})$ with $\Sigma_{\boldsymbol{\theta}_z^{(g)}} = \left(Z^{(g)T} \Omega^* Z^{(g)} + \frac{I_n}{\sigma_{\zeta_z^{(g)}}^2} \right)^{-1}$ and $\boldsymbol{\mu}_{\boldsymbol{\theta}_z^{(g)}} = \Sigma_{\boldsymbol{\theta}_z^{(g)}} \left\{ Z^{(g)T} \Omega^* \left(\boldsymbol{\lambda} - X \boldsymbol{\delta}_z - Z^{(r)} \boldsymbol{\theta}_z^{(r)} \right) + \frac{V \boldsymbol{\eta}_z^{(g)}}{\sigma_{\zeta_z^{(g)}}^2} \right\}$; we implement a sum-to-zero constraint *on the fly* for these parameters (Besag et al., 1995; Berrocal et al., 2012; Warren et al., 2021);
- $f(\boldsymbol{\theta}_z^{(r)} | \boldsymbol{\Theta}_{-\boldsymbol{\theta}_z^{(r)}}, \mathbf{Y})$ has similar form to $f(\boldsymbol{\theta}_z^{(g)} | \boldsymbol{\Theta}_{-\boldsymbol{\theta}_z^{(g)}}, \mathbf{Y})$ with (g) replaced by (r) ;
- $\sigma_{\zeta_z^{(g)}}^2 | \boldsymbol{\Theta}_{-\sigma_{\zeta_z^{(g)}}^2}, \mathbf{Y} \sim \text{Inverse Gamma} \left(\frac{n}{2} + 0.01, \frac{(\boldsymbol{\theta}_z^{(g)} - V \boldsymbol{\eta}_z^{(g)})^T (\boldsymbol{\theta}_z^{(g)} - V \boldsymbol{\eta}_z^{(g)})}{2} + 0.01 \right);$
- $f(\sigma_{\zeta_z^{(r)}}^2 | \boldsymbol{\Theta}_{-\sigma_{\zeta_z^{(r)}}^2}, \mathbf{Y})$, $f(\sigma_{\zeta_w^{(g)}}^2 | \boldsymbol{\Theta}_{-\sigma_{\zeta_w^{(g)}}^2}, \mathbf{Y})$, and $f(\sigma_{\zeta_w^{(r)}}^2 | \boldsymbol{\Theta}_{-\sigma_{\zeta_w^{(r)}}^2}, \mathbf{Y})$ each have the same form as $f(\sigma_{\zeta_z^{(g)}}^2 | \boldsymbol{\Theta}_{-\sigma_{\zeta_z^{(g)}}^2}, \mathbf{Y})$ with (g) replaced by (r) and w replaced by z when appropriate;

- $\boldsymbol{\eta}_z^{(g)} | \Theta_{-\boldsymbol{\eta}_z^{(g)}}, \mathbf{Y} \sim \text{MVN} \left(\Sigma_{\boldsymbol{\eta}_z^{(g)}}, \boldsymbol{\mu}_{\boldsymbol{\eta}_z^{(g)}} \right)$ with $\Sigma_{\boldsymbol{\eta}_z^{(g)}} = \left\{ \frac{V^T V}{\sigma_{\zeta_z^{(g)}}^2} + (\Sigma_{11} - \Sigma_{12} \Sigma_{22}^{-1} \Sigma_{21})^{-1} \right\}^{-1}$
 and $\boldsymbol{\mu}_{\boldsymbol{\eta}_z^{(g)}} = \Sigma_{\boldsymbol{\eta}_z^{(g)}} \left\{ \frac{V^T \boldsymbol{\theta}_z^{(g)}}{\sigma_{\zeta_z^{(g)}}^2} + (\Sigma_{11} - \Sigma_{12} \Sigma_{22}^{-1} \Sigma_{12})^{-1} \Sigma_{12} \Sigma_{22}^{-1} \begin{bmatrix} \boldsymbol{\eta}_z^{(r)} \\ \boldsymbol{\eta}_w^{(g)} \\ \boldsymbol{\eta}_w^{(r)} \end{bmatrix} \right\}$, where $\Sigma_{11} = \Omega_{11} \Sigma(\phi)$,
 $\Sigma_{12} = \{\Omega_{12} \Sigma(\phi), \Omega_{13} \Sigma(\phi), \Omega_{14} \Sigma(\phi)\}$, $\Sigma_{21} = \Sigma_{12}^T$, and $\Sigma_{22} = \Omega_{2:4,2:4} \otimes \Sigma(\phi)$;
- $f \left(\boldsymbol{\eta}_z^{(r)} | \Theta_{-\boldsymbol{\eta}_z^{(r)}}, \mathbf{Y} \right)$, $f \left(\boldsymbol{\eta}_w^{(g)} | \Theta_{-\boldsymbol{\eta}_w^{(g)}}, \mathbf{Y} \right)$, and $f \left(\boldsymbol{\eta}_w^{(r)} | \Theta_{-\boldsymbol{\eta}_w^{(r)}}, \mathbf{Y} \right)$ each have a similar form to $f \left(\boldsymbol{\eta}_z^{(g)} | \Theta_{-\boldsymbol{\eta}_z^{(g)}}, \mathbf{Y} \right)$ with the obvious (g) , (r) , z , w changes and updates of the subscripts on the entries of Ω and ordering of the vectors;
- $w_{ij} | \Theta_{-w_{ij}}, \mathbf{Y}_{\{Y_{ij} > 0\}} \equiv \text{logit}(Y_{ij})$;
- $w_{ij} | \Theta_{-w_{ij}}, \mathbf{Y}_{\{Y_{ij} = 0\}} \stackrel{\text{ind}}{\sim} \text{N} \left(\mathbf{x}_{ij}^T \boldsymbol{\beta}_w + \mathbf{d}_j^T \boldsymbol{\gamma}_w^{(g)} + \mathbf{d}_i^T \boldsymbol{\gamma}_w^{(r)} + \theta_{wj}^{(g)} + \theta_{wi}^{(r)}, \sigma_\epsilon^2 \right)$;
- $\boldsymbol{\delta}_w | \Theta_{-\boldsymbol{\delta}_w}, \mathbf{Y} \sim \text{MVN} \left(\Sigma_{\boldsymbol{\delta}_w}, \boldsymbol{\mu}_{\boldsymbol{\delta}_w} \right)$ with $\Sigma_{\boldsymbol{\delta}_w} = \left(\frac{X^T X}{\sigma_\epsilon^2} + \frac{I_{(p_x + 2p_d)}}{100^2} \right)^{-1}$ and
 $\boldsymbol{\mu}_{\boldsymbol{\delta}_w} = \frac{\Sigma_{\boldsymbol{\delta}_w} X^T (\mathbf{w} - Z^{(g)} \boldsymbol{\theta}_w^{(g)} - Z^{(r)} \boldsymbol{\theta}_w^{(r)})}{\sigma_\epsilon^2}$;
- $\sigma_\epsilon^2 | \Theta_{-\sigma_\epsilon^2}, \mathbf{Y} \sim$
 Inverse Gamma $\left(\frac{n^*}{2} + 0.01, \frac{(\mathbf{w} - X \boldsymbol{\delta}_w - Z^{(g)} \boldsymbol{\theta}_w^{(g)} - Z^{(r)} \boldsymbol{\theta}_w^{(r)})^T (\mathbf{w} - X \boldsymbol{\delta}_w - Z^{(g)} \boldsymbol{\theta}_w^{(g)} - Z^{(r)} \boldsymbol{\theta}_w^{(r)})}{2} + 0.01 \right)$;
- $\boldsymbol{\theta}_w^{(g)} | \Theta_{-\boldsymbol{\theta}_w^{(g)}}, \mathbf{Y} \sim \text{MVN} \left(\Sigma_{\boldsymbol{\theta}_w^{(g)}}, \boldsymbol{\mu}_{\boldsymbol{\theta}_w^{(g)}} \right)$ with $\Sigma_{\boldsymbol{\theta}_w^{(g)}} = \left(\frac{Z^{(g)T} Z^{(g)}}{\sigma_\epsilon^2} + \frac{I_n}{\sigma_{\zeta_w^{(g)}}^2} \right)^{-1}$ and $\boldsymbol{\mu}_{\boldsymbol{\theta}_w^{(g)}} =$
 $\Sigma_{\boldsymbol{\theta}_w^{(g)}} \left\{ \frac{Z^{(g)T} (\mathbf{w} - X \boldsymbol{\delta}_w - Z^{(r)} \boldsymbol{\theta}_w^{(r)})}{\sigma_\epsilon^2} + \frac{V \boldsymbol{\eta}_w^{(g)}}{\sigma_{\zeta_w^{(g)}}^2} \right\}$; we implement a sum-to-zero constraint *on the fly* for these parameters;
- $f \left(\boldsymbol{\theta}_w^{(r)} | \Theta_{-\boldsymbol{\theta}_w^{(r)}}, \mathbf{Y} \right)$ has the same as $f \left(\boldsymbol{\theta}_w^{(g)} | \Theta_{-\boldsymbol{\theta}_w^{(g)}}, \mathbf{Y} \right)$ with (g) replaced by (r) ;
- $\Omega^{-1} | \Theta_{-\Omega^{-1}}, \mathbf{Y} \sim \text{Wishart} \left\{ \left(\sum_{j=1}^m \sum_{i=1}^m \boldsymbol{\eta}(\mathbf{s}_j^*) \boldsymbol{\eta}(\mathbf{s}_i^*)^T \Sigma(\phi)_{ij}^{-1} + I_4 \right)^{-1}, m + 5 \right\}$; and
- $f \{ \ln(\phi) | \text{rest} \} \propto |\Sigma(\phi)^{-1}|^2 \exp \left[-\frac{1}{2} \boldsymbol{\eta}^T \{ \Sigma(\phi)^{-1} \otimes \Omega^{-1} \} \boldsymbol{\eta} \right] f \{ \ln(\phi) \}$; as in Section S.1, we work with $\ln(\phi) \in \mathbb{R}$ instead of ϕ so that a symmetric proposal density can be used in the Metropolis algorithm.

S2 Additional figures and tables

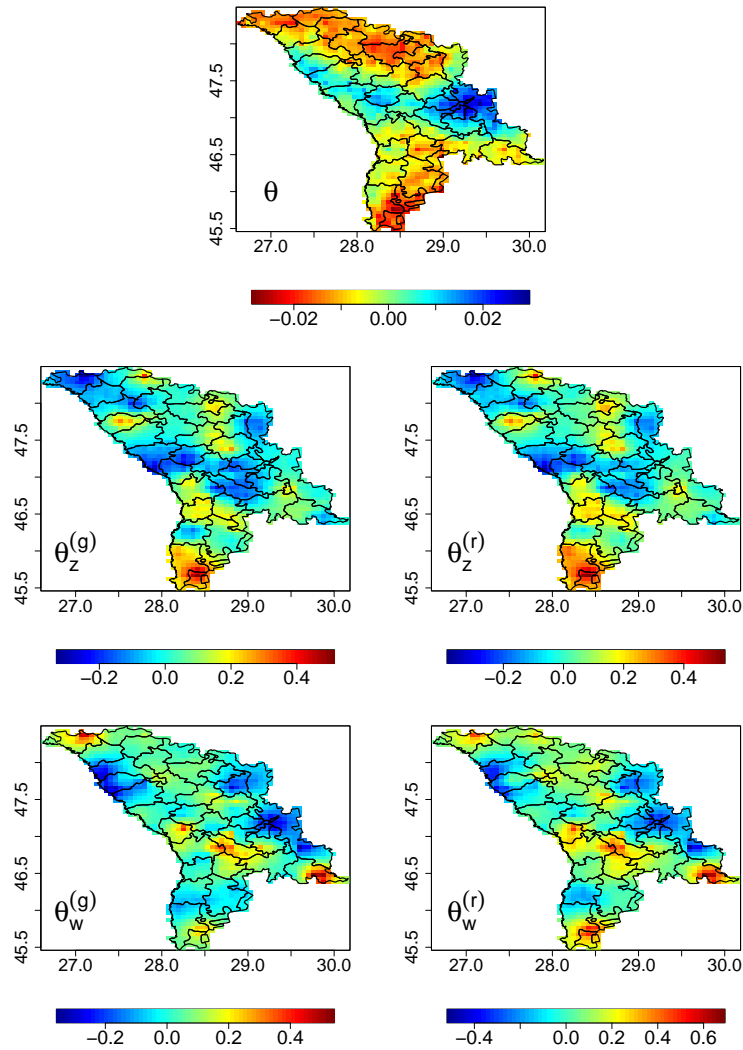


Figure S1: Predicted random effect parameter results (posterior means) from the Republic of Moldova data analyses. Patristic distance results (top row); transmission probability results (rows two and three). z : binary component; w : continuous component; g : giver role; r : receiver role.

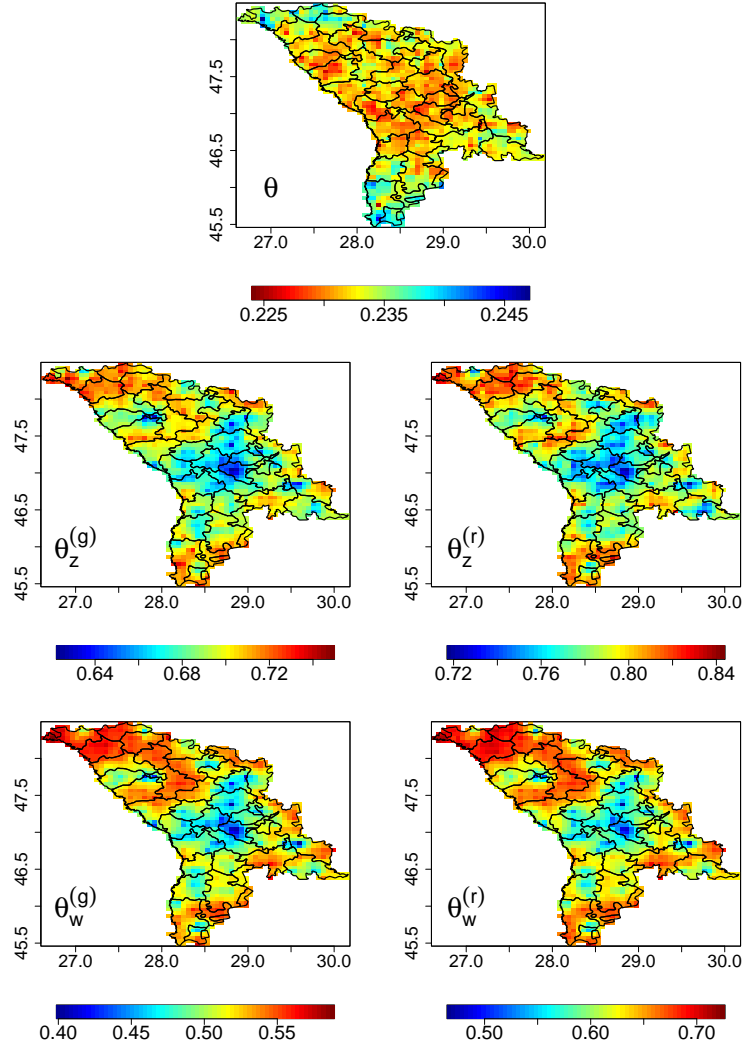


Figure S2: Predicted random effect parameter results (posterior standard deviations) from the Republic of Moldova data analyses. Patristic distance results (top row); transmission probability results (rows two and three). z : binary component; w : continuous component; g : giver role; r : receiver role.

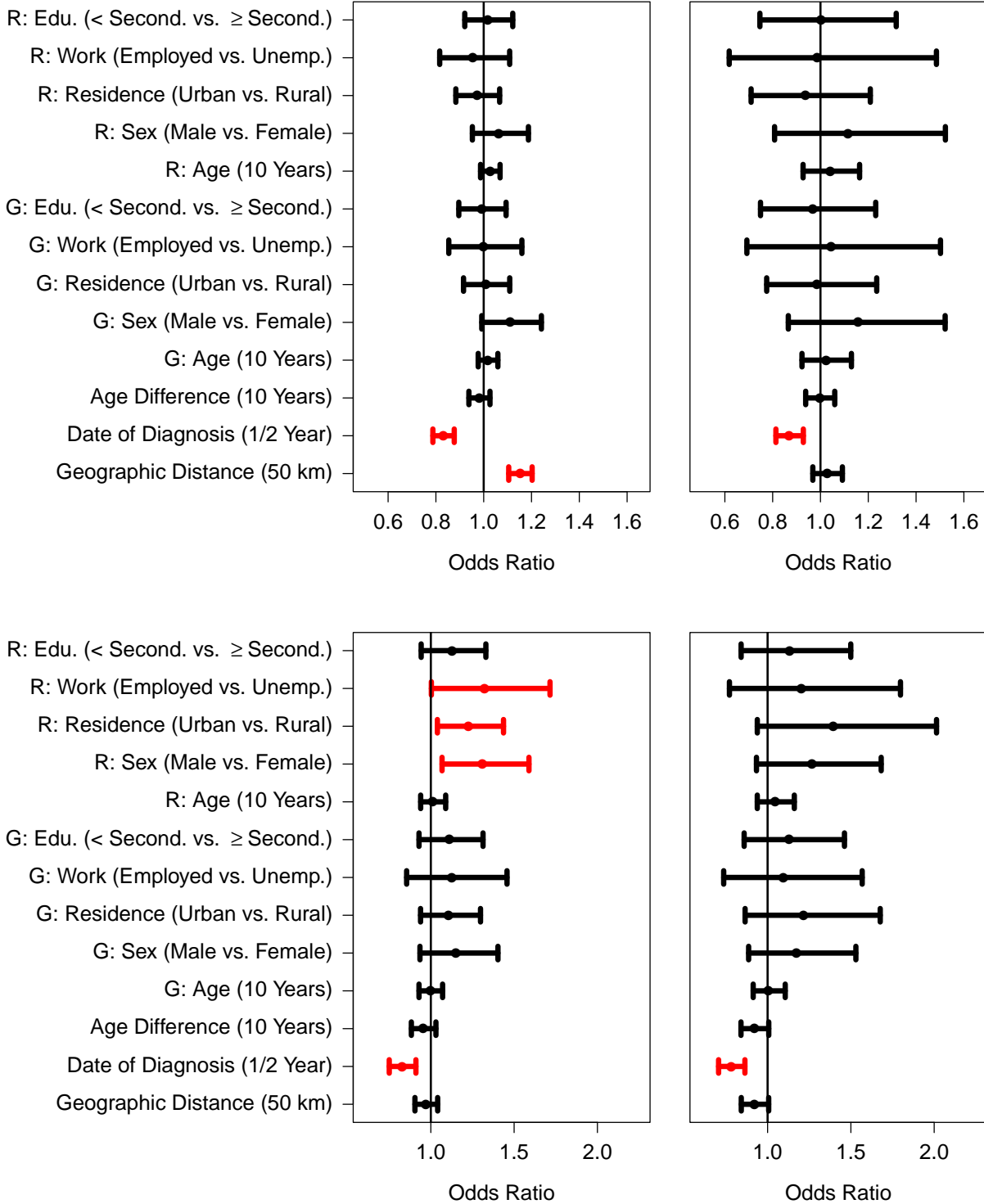


Figure S3: Results from the transmission probability analyses in the Republic of Moldova. Posterior means and 95% equal-tailed quantile-based credible intervals are shown for the binary component (top row) and continuous component (bottom row) exponentiated regression parameters from the standard model (left column) and new method (right column). Red lines indicate that the interval excludes one. Estimates from the “Same Village” indicator parameter are omitted due to differing scales (see Table 5 of the main text for complete information).

Table S1: Simulation study true parameter values obtained from the Republic of Moldova data analyses. Posterior means are presented unless otherwise noted with * (posterior medians). PD: patristic distances; TP: transmission probabilities; z : binary component; w : continuous component; g : giver role; r : receiver role.

Parameter	PD	TP (z, g)	TP (z, r)	TP (w, g)	TP (w, r)
Intercept	-8.1265	-1.2473		-7.6764	
Distance Between Villages	0.0026	0.0290		-0.0877	
Same Village	-0.5921	1.3623		3.7810	
Date of Diagnosis Distance	0.0039	-0.1206		-0.2114	
Age Difference	0.0003	-0.0028		-0.0840	
Age	-0.0088	0.0265	0.0455	0.0047	0.0501
Sex (Male vs. Female):		0.1366	0.0959	0.1506	0.2248
Mixed Pair vs. Both Female	-0.0171				
Both Male vs. Both Female	-0.0215				
Residence Location (Urban vs. Rural):		-0.0213	-0.0742	0.1817	0.3135
Mixed Pair vs. Both Rural	-0.0224				
Both Urban vs. Both Rural	-0.0348				
Working Status (Employed vs. Unemployed):		0.0245	-0.0387	0.0712	0.1605
Mixed Pair vs. Both Unemployed	-0.0216				
Both Employed vs. Both Unemployed	-0.0170				
Education (< Secondary vs. \geq Secondary):		-0.0403	-0.0081	0.1127	0.1128
Mixed Pair vs. Both \geq Secondary	0.0503				
Both < Secondary vs. Both \geq Secondary	0.1058				
σ_ϵ^2	0.0548			3.7514	
σ_ζ^2	0.0504	0.2552	0.3482	0.0231	0.0215
τ^2*	0.0107				
ϕ^*	0.4110		7.8202		
Ω_{11}^*			0.2535		
Ω_{22}^*			0.3038		
Ω_{33}^*			0.2980		
Ω_{44}^*			0.4674		
Ω_{12}^*			0.2043		
Ω_{13}^*			-0.0045		
Ω_{14}^*			0.0643		
Ω_{23}^*			-0.0012		
Ω_{24}^*			0.0737		
Ω_{34}^*			0.2978		

References

- Berrocal, V. J., A. E. Gelfand, and D. M. Holland (2012). Space-time data fusion under error in computer model output: an application to modeling air quality. *Biometrics* 68(3), 837–848.
- Besag, J., P. Green, D. Higdon, K. Mengersen, et al. (1995). Bayesian computation and stochastic systems. *Statistical science* 10(1), 3–41.
- Gelfand, A. E. and A. F. Smith (1990). Sampling-based approaches to calculating marginal densities. *Journal of the American Statistical Association* 85(410), 398–409.
- Geman, S. and D. Geman (1984). Stochastic relaxation, Gibbs distributions, and the Bayesian restoration of images. *IEEE Transactions on Pattern Analysis and Machine Intelligence PAM1-6*(6), 721–741.
- Makalic, E. and D. Schmidt (2021). High-dimensional Bayesian regularised regression with the bayesreg package. Most recent version: Dec. 2016.
- Metropolis, N., A. W. Rosenbluth, M. N. Rosenbluth, A. H. Teller, and E. Teller (1953). Equation of state calculations by fast computing machines. *The Journal of Chemical Physics* 21(6), 1087–1092.
- Polson, N. G., J. G. Scott, and J. Windle (2013). Bayesian inference for logistic models using Pólya–Gamma latent variables. *Journal of the American Statistical Association* 108(504), 1339–1349.
- Warren, J. L., M. L. Miranda, J. L. Tootoo, C. E. Osgood, and M. L. Bell (2021). Spatial distributed lag data fusion for estimating ambient air pollution. *The Annals of Applied Statistics* 15(1), 323–342.